

Stationary waves for nonlinear seismic wave propagation

Leo Dostal^a, Marten Hollm^a, Andrei V. Metrikine^b, Apostolos Tsouvalas^b,
Karel N. van Dalen^b

^a*Institute of Mechanics and Ocean Engineering, Hamburg University of Technology,
21073 Hamburg, Germany*

^b*Faculty of Civil Engineering & Geosciences, TU Delft, Delft, Netherlands*

Abstract

In this work, new equations for seismic wave propagation of shear waves in a nonlocal, history-dependent nonlinear medium are established. The development of these equations came up due to the necessity of accurate modelling for the study of stationary seismic wave propagation. Based on this model, stationary waves are determined. Then, a fully implicit numerical scheme is developed and used for the numerical computation of wave propagation starting from Gaussian pulses. Moreover, the propagation of stationary waves is shown in space and time. Finally, collision of the determined stationary waves is shown in order to examine, whether the obtained stationary waves are solitons.

Keywords: seismic waves, nonlinear waves, stationary waves

1. Introduction

For the prediction of the so-called site response - the response of the top soil layers of the earth - induced by seismic waves, typically 1-D models are employed. The so-called equivalent linear scheme is used very often, in which the soil stiffness and damping are modelled taking constant shear modulus and material damping ratio, respectively. The actual values of the shear modulus and damping ratio are based on the maximum level of strain in each layer of the soil profile; this requires iteration as it is not possible to determine the maximum strain level beforehand. For high maximum strain levels in the soil layers, such equivalent shear modulus and damping ratio for each layer cannot accurately represent the behavior over the entire duration of a seismic event, as the strains vary significantly. In these cases, a nonlinear

time domain solution is typically used to account for the variation of the shear modulus and damping ratio during shaking (e.g., Régnier et al. [1]).

Contemporary research into nonlinear time-domain models for seismic site response analysis is mostly focused on the development of advanced constitutive models so as to capture important features of soil behavior such as anisotropy, pore water pressure generation, and dilation [2]. However, limited research has been devoted to the fundamental nonlinear-dynamics aspects of the seismic site response. For the commonly used hyperbolic constitutive model [3], softening behaviour and super-harmonic resonances were recently demonstrated for a superficial soil layer under uniform periodic excitation at the lower boundary in the one dimensional case [4]. However, the possibility for stationary waves to propagate through the soil column and reach the surface has not been widely recognized in the seismological literature and neither in the geo-technical literature.

In this paper, we therefore investigate the existence of stationary waves in a shallow soil layer (located at a depth of a few hundreds of meters) with the constitutive behaviour governed by the hyperbolic model, implying that the shear modulus is strain dependent. As the classical wave equation with this particular nonlinearity appears to have non-physical discontinuous solutions as different parts of an initial condition propagate with different speeds, which is related to the fact that associated characteristics are crossing, leading to a gradient catastrophe [5]. Therefore, we extend the nonlinear classical model to a nonlinear *gradient elasticity model*, which sometimes is also called a *higher-order gradient continuum*. The classical stress-strain relation is extended with additional gradients to capture the effect of small-scale soil heterogeneity and yet keeping the description of the material homogeneous, which introduces dispersive effects particularly for the shorter waves [6]. Such higher-order gradients naturally occur when applying homogenization techniques for periodically inhomogeneous media; cf. Eq. 10 of Metrikine [6]. Dispersive effects do have significant effects on the behaviour of stationary waves, as such waves exist exactly because of the balance between dispersive and nonlinear effects allowing their propagation without distortion. The dispersion also prohibits the formation of jumps, which leads to physically realisable stationary wave solutions. So-called higher-order dispersion correction and higher-order dispersive nonlinearity has been discussed in the context of the well-known Korteweg-de Vries equation [7].

Sticking to the 1-D assumption, we derive the equation of motion for the soil medium using Newton's second law and Eringen's general stress-

strain relation [8], which allows to introduce the higher-order derivatives in a consistent manner. For simplicity, the strain dependence of all elastic constants is chosen according to the mentioned hyperbolic model. We derive stationary solutions for the obtained equation of motion of the nonlinear gradient elasticity model; the stationary wave solution is found by selecting the *homoclinic orbit* in the phase plane. In addition, we present a novel numerical scheme that can be used to solve the equation of motion. It is used to validate the obtained stationary wave solution. Finally, it is demonstrated that the stationary-wave solution is in fact not a true *soliton* by creating two colliding stationary waves (i.e., propagating in opposite direction and passing each other). After interaction, their original shape is not retained.

2. Modelling

The starting point to derive the equation of motion is Newton's second law. For transverse waves propagating in the z direction (one-dimensional situation), it reads [9]

$$\rho \frac{\partial^2 u}{\partial t^2} = \frac{\partial \sigma_{zx}}{\partial z}, \quad (1)$$

where $u(z, t)$ is the horizontal displacement (in the x direction), t is time, and σ_{zx} is the shear stress (on z plane, pointing in x direction). In a nonlinear system, the stress-strain relation generally reads as follows

$$\sigma_{zx}(z, t) = \int_{-\infty}^{\infty} \int_{-\infty}^{\infty} g(z - \zeta, t - \tau, \gamma(\zeta, \tau)) \varepsilon_{zx}(\zeta, \tau) d\zeta d\tau, \quad (2)$$

which expresses that the stress σ_{zx} at location z and time t generally depends on the strain ε_{zx} at all points of the medium, and on the entire strain history (note that ζ and τ denotes auxiliary space and time variables). The specific nonlocality and history dependence is contained in the kernel function $g(z, t, \gamma)$. Moreover, the strain depends on the displacement in the following way [9]

$$\varepsilon_{zx} = \frac{1}{2} \frac{\partial u}{\partial z}. \quad (3)$$

The nonlinearity comes into play through the γ dependence of the kernel function, which expresses that the elasticity operators are strain dependent.

In this work, we relate γ to the deviatoric component of the so-called octahedral strain [10], which for the one-dimensional case leads to

$$\gamma = \sqrt{3}|\varepsilon_{zx}| = \frac{\sqrt{3}}{2} \left| \frac{\partial u}{\partial z} \right|. \quad (4)$$

2.1. Nonlocal, history-dependent nonlinear medium

In principle, the distribution of the kernel function $g(z, t, \gamma)$ in z and t is arbitrary, leading to an equation of motion of the integro-differential type once Eq. (2) is substituted into Eq. (1). However, it is well-known (e.g., [11]) that particular nonlocal and history effects can be captured solely by higher-order derivatives in the equation of motion. In this paper, we will restrict our-selves to such type of nonlocality and history dependence. Therefore, we assume

$$g(z - \zeta, t - \tau, \gamma) = 2 \left(G(\gamma) \delta(z - \zeta) \delta(t - \tau) - L^2 G^{(L)}(\gamma) \delta''(z - \zeta) \delta(t - \tau) + T^2 G^{(T)}(\gamma) \delta(z - \zeta) \ddot{\delta}(t - \tau) \right), \quad (5)$$

where T and L denote time and length scales characterizing the history dependence and the nonlocality, respectively, $G(\gamma)$ is the nonlinear shear modulus, $G^{(L,T)}(\gamma)$ are additional elastic coefficients (related to higher-order derivatives, as shown below), and $\gamma = \gamma(\zeta, \tau)$; $\delta(\dots)$ denotes Dirac's delta function, an overdot signifies differentiation with respect to τ , and a prime differentiation with respect to ζ . It is emphasized that all elastic coefficients in Eq. (5) are strain dependent.

Now, inserting Eq. (5) into the Eq. (2), we obtain the stress-strain relation of a nonlinear higher-order gradient continuum

$$\sigma_{zx}(z, t) = 2 \left(G(\gamma) \varepsilon_{zx}(\zeta, t) - L^2 \frac{\partial^2}{\partial \zeta^2} (G^{(L)}(\gamma) \varepsilon_{zx}(\zeta, t)) + T^2 \frac{\partial^2}{\partial t^2} (G^{(T)}(\gamma) \varepsilon_{zx}(\zeta, t)) \right). \quad (6)$$

Substituting the expressions (3) and (6) into (1) yields the corresponding equation of motion

$$\rho \frac{\partial^2}{\partial t^2} u = \frac{\partial}{\partial z} \left(G(\gamma) \frac{\partial}{\partial z} u - L^2 \frac{\partial^2}{\partial z^2} \left(G^{(L)}(\gamma) \frac{\partial}{\partial z} u \right) + T^2 \frac{\partial^2}{\partial t^2} \left(G^{(T)}(\gamma) \frac{\partial}{\partial z} u \right) \right). \quad (7)$$

For simplicity, we relate the (strain-dependent) additional elastic coefficients $G^{(L,T)}(\gamma)$ to the conventional strain-dependent shear modulus $G(\gamma)$ using dimensionless constants B_1 and B_2

$$\begin{aligned} G^{(L)}(\gamma) &= B_1 G(\gamma), \\ G^{(T)}(\gamma) &= B_2 G(\gamma). \end{aligned} \tag{8}$$

We also interrelate the characteristic length and time scales: $T^2 = \rho L^2 / c_0^2$ with $c_0^2 = G_0 / \rho$, where ρ denotes the material density, G_0 the well-known small-strain shear modulus from linear elasticity, and c_0 the corresponding shear-wave speed. Using these choices, the equation of motion (Eq. (7)) can be written as

$$\rho \frac{\partial^2}{\partial t^2} u = \frac{\partial}{\partial z} \left(G(\gamma) \frac{\partial}{\partial z} u - B_1 L^2 \frac{\partial^2}{\partial z^2} \left(G(\gamma) \frac{\partial}{\partial z} u \right) + B_2 \frac{\rho L^2}{G_0} \frac{\partial^2}{\partial t^2} \left(G(\gamma) \frac{\partial}{\partial z} u \right) \right). \tag{9}$$

In this work, we use the hyperbolic soil model

$$G(\gamma) = \frac{G_0}{1 + \left(\frac{\gamma}{\gamma_{\text{ref}}} \right)^\beta}, \quad \gamma \geq 0, \tag{10}$$

for the nonlinear shear modulus $G(\gamma)$, which was introduced by Hardin and Drnevich [12]. Thereby, γ_{ref} is the reference shear strain and β is dimensionless constant ($0 < \beta < 1$).

2.2. Nonlocal, history-dependent linear medium

History dependence and nonlocality can to some extent still be represented using Dirac functions in the kernel function $g(z, t)$, but only if derivatives are included. In the specific case of a nonlocally reacting and history-dependent linear medium, the kernel function could be chosen as (the primes denote derivatives with respect to ζ , while overdots indicate derivatives with respect to τ)

$$\begin{aligned} g(z - \zeta, t - \tau, \gamma) &= 2(G_0 \delta(z - \zeta) \delta(t - \tau) - L^2 G_0^{(L)} \delta''(z - \zeta) \delta(t - \tau) \\ &\quad + T^2 G_0^{(T)} \delta(z - \zeta) \ddot{\delta}(t - \tau)), \end{aligned} \tag{11}$$

where T and L again denote time and length scales characterizing the history dependence and the nonlocality, respectively, while $G_0^{(L)}$ and $G_0^{(T)}$ are

the additional elastic constants (associated with the higher-order derivatives); the subscript “0” indicates that the corresponding coefficient relates to small-strain (i.e., linear) behavior. Using Eq. (11), the stress-strain relation (Eq. (2)) reduces to the one of the linear higher-order gradient continuum:

$$\sigma_{zx}(z, t) = 2 \left(G_0 \varepsilon_{zx}(\zeta, t) - L^2 G_0^{(L)}(\gamma) \varepsilon_{zx}''(\zeta, t) + T^2 G_0^{(T)} \ddot{\varepsilon}_{zx}(\zeta, t) \right). \quad (12)$$

The corresponding equation of motion reads

$$\rho \frac{\partial^2}{\partial t^2} u = G_0 \frac{\partial^2}{\partial z^2} u - L^2 G_0^{(L)} \frac{\partial^4}{\partial z^4} u + T^2 G_0^{(T)} \frac{\partial^4}{\partial z^2 \partial t^2} u, \quad (13)$$

where the expressions

$$\begin{aligned} G_0^{(L)} &= B_1 G_0, \\ G_0^{(T)} &= \frac{\rho L^2 B_2}{T^2} = B_2 G_0, \end{aligned} \quad (14)$$

can be substituted in order to relate the elastic constants $G_0^{(L)}$ and $G_0^{(T)}$ to the small-strain shear modulus G_0 by means of the dimensionless coefficients B_1 and B_2 .

The nonlinear equation (9) reduces to the linear one (Eq. (13)), if the strain dependence is ignored (i.e., $G(\gamma) \rightarrow G_0$). The linear equation (13) has been considered before in Metrikine [6] as a gradient elasticity model.

It was derived by Metrikine and Askes [13] from a discrete model using a continualization procedure and later used, for example, by Georgiadis et al. [14].

If the linear system has no memory (i.e., is history independent) and the behavior is completely local, the kernel function contains Dirac functions. For example, in the case of a classical continuum (G_0 denotes the small-strain shear modulus)

$$g(z - \zeta, t - \tau, \gamma) = 2G_0 \delta(z - \zeta) \delta(t - \tau), \quad (15)$$

which leads to the conventional stress-strain relation,

$$\sigma_{zx}(z, t) = 2G_0 \varepsilon_{zx}(\zeta, t), \quad (16)$$

and the associated equation of motion (which is a classical wave equation):

$$\rho \frac{\partial^2}{\partial t^2} u = G_0 \frac{\partial^2}{\partial z^2} u. \quad (17)$$

3. Stationary wave solutions

It is possible to determine solutions to equation of motion (9) for a non-local, history-dependent nonlinear medium. We seek solutions, which do not change their shape while propagating in the nonlinear medium. This means that, starting at an initial condition, the stationary solution to equation (9) does not change with respect to the coordinate $\xi = z - ct$, which moves with the velocity $c \in \mathbb{R}$. Thereby, c can be arbitrarily chosen and leads to a specific solution. The transformation $\xi = z - ct$ and $()_\xi := \frac{\partial}{\partial \xi}$ yields

$$u_{tt} = u_{\xi\xi}c^2, \quad u_{ttt} = u_{\xi\xi\xi}c^2, \quad u_{zt} = u_{\xi\xi}c, \quad \text{and} \quad \frac{\partial}{\partial \xi} = \frac{\partial}{\partial z} \quad (18)$$

where the subscripts

$$()_t := \frac{\partial}{\partial t}, \quad ()_z := \frac{\partial}{\partial z}, \quad ()_\xi := \frac{\partial}{\partial \xi} \quad (19)$$

are used here and in the following. Substituting expressions (18) into Eq. (9) we get the ordinary differential equation

$$\rho c^2 u_{\xi\xi} = \frac{\partial}{\partial \xi} \left(G(\gamma)u_\xi + \left(B_2 c^2 \frac{\rho L^2}{G_0} - B_1 L^2 \right) \frac{\partial^2}{\partial \xi^2} (G(\gamma)u_\xi) \right). \quad (20)$$

In order to evaluate $\frac{\partial^2}{\partial \xi^2} (G(\gamma)u_\xi)$ in Eq. (20) for the hyperbolic soil model from Eq. (10), it has to be noted that the absolute value function $g(x) = |x|$ is not for $x = 0$. But it is weakly differentiable with $\text{sgn}(x)$ as weak derivative,

which denotes the sign function. Using this, we specifically obtain

$$\begin{aligned}
\rho c^2 u_{\xi\xi} = & \frac{\partial}{\partial \xi} \left[u_{\xi} \frac{G_0}{1 + \left(\frac{\sqrt{3}|u_{\xi}|}{2\gamma_{\text{ref}}} \right)^{\beta}} + (B_2 c^2 \rho L^2 - G_0 B_1 L^2) \left\{ u_{\xi\xi\xi} \left(\frac{1}{1 + \left(\frac{\sqrt{3}|u_{\xi}|}{2\gamma_{\text{ref}}} \right)^{\beta}} \right. \right. \right. \\
& - \beta \left(\frac{\sqrt{3}|u_{\xi}|}{2\gamma_{\text{ref}}} \right)^{\beta} \left(1 + \left(\frac{\sqrt{3}|u_{\xi}|}{2\gamma_{\text{ref}}} \right)^{\beta} \right)^{-2} \\
& + \frac{\sqrt{3} \operatorname{sgn}(u_{\xi})}{2\gamma_{\text{ref}}} u_{\xi\xi}^2 \left(2\beta^2 \left(\frac{\sqrt{3}|u_{\xi}|}{2\gamma_{\text{ref}}} \right)^{2\beta-1} \left(1 + \left(\frac{\sqrt{3}|u_{\xi}|}{2\gamma_{\text{ref}}} \right)^{\beta} \right)^{-3} \right. \\
& \left. \left. \left. - (\beta + \beta^2) \left(\frac{\sqrt{3}|u_{\xi}|}{2\gamma_{\text{ref}}} \right)^{\beta-1} \left(1 + \left(\frac{\sqrt{3}|u_{\xi}|}{2\gamma_{\text{ref}}} \right)^{\beta} \right)^{-2} \right) \right\} \right]
\end{aligned} \tag{21}$$

Integration of Eq. (21) with respect to ξ , rearrangement with respect to $u_{\xi\xi\xi}$, and setting $y = u_{\xi}$, $(\cdot) := \frac{\partial}{\partial \xi}$ yields

$$\begin{aligned}
\ddot{y} = & \frac{1}{1 - \beta \left(\frac{\sqrt{3}|y|}{2\gamma_{\text{ref}}} \right)^{\beta} \left(1 + \left(\frac{\sqrt{3}|y|}{2\gamma_{\text{ref}}} \right)^{\beta} \right)^{-1}} \left\{ \frac{\rho c^2 \left(1 + \left(\frac{\sqrt{3}|y|}{2\gamma_{\text{ref}}} \right)^{\beta} \right) - G_0}{B_2 c^2 \rho L^2 - G_0 B_1 L^2} y \right. \\
& - \frac{\sqrt{3} \operatorname{sgn}(y)}{2\gamma_{\text{ref}}} \left[2\beta^2 \left(\frac{\sqrt{3}|y|}{2\gamma_{\text{ref}}} \right)^{2\beta-1} \left(1 + \left(\frac{\sqrt{3}|y|}{2\gamma_{\text{ref}}} \right)^{\beta} \right)^{-2} \right. \\
& \left. \left. - (\beta + \beta^2) \left(\frac{\sqrt{3}|y|}{2\gamma_{\text{ref}}} \right)^{\beta-1} \left(1 + \left(\frac{\sqrt{3}|y|}{2\gamma_{\text{ref}}} \right)^{\beta} \right)^{-1} \right] \dot{y}^2 \right\}.
\end{aligned} \tag{22}$$

This is a nonlinear second order ordinary differential equation, which can be solved for a stationary wave solution of Eq. (9)

4. Numerical scheme

In order to solve eq. (9), we have developed a fully implicit scheme for the numerical computation of PDE's of the form

$$\begin{aligned} \frac{\partial^2 u}{\partial t^2} = & \frac{\partial}{\partial z} \left(G \left(\frac{\partial u}{\partial z} \right) \frac{\partial u}{\partial z} - B_1 L^2 \frac{\partial^2}{\partial z^2} \left(G \left(\frac{\partial u}{\partial z} \right) \frac{\partial u}{\partial z} \right) \right. \\ & \left. + B_2 \frac{\rho L^2}{G_0} \frac{\partial^2}{\partial t^2} \left(G \left(\frac{\partial u}{\partial z} \right) \frac{\partial u}{\partial z} \right) \right). \end{aligned} \quad (23)$$

It is assumed that the solution $u(t, z)$ of eq. (9) exists in time $t \in [0, T]$ and space $z \in [Z_\ell, Z_h]$. Therefore, a grid in time

$$0 = t_0 < t_1 < \dots < t_N = T, \quad t_n = n\Delta t \text{ for } n = 0, \dots, N, \quad \Delta t = \frac{T}{N} \quad (24)$$

and grid in space

$$Z_\ell = z_0 < z_1 < \dots < z_M = Z_h, \quad z_i = i\Delta z \text{ for } i = 0, \dots, M, \quad \Delta z = \frac{Z_\ell - Z_h}{M} \quad (25)$$

is introduced. Using

$$h(u_z) := G(\gamma) u_z, \quad (26)$$

Eq. (9) can be written as

$$\rho u_{tt} = h_z - B_1 L^2 h_{zzz} + B_2 \frac{\rho L^2}{G_0} h_{ttz}. \quad (27)$$

Assuming that the solution is known at the timepoints t_{n-1} and t_n and replacing the time derivative by finite differences, Eq. (27) results into the nonlinear equation

$$f(u^{n+1})(z_i) = 0 \quad (28)$$

with

$$u^{n+1} = [u_0^{n+1}, u_1^{n+1}, \dots, u_M^{n+1}]^T \quad (29)$$

and

$$\begin{aligned} f(u^{n+1})(z_i) = & \rho \frac{u_i^{n+1} - 2u_i^n + u_i^{n-1}}{\Delta t^2} - h_z(u_{z,i}^{n+1}) + B_1 L^2 h_{zzz}(u_{z,i}^{n+1}) \\ & - B_2 \frac{\rho L^2}{G_0} \frac{h_z(u_{z,i}^{n+1}) - 2h_z(u_{z,i}^n) + h_z(u_{z,i}^{n-1})}{\Delta t^2}. \end{aligned} \quad (30)$$

Thereby, u_i^n is a grid function approximating the solution at time t_n and space z_i , i.e. $u_i^n \approx u(t_n, z_i)$, and $u_{z,i}^n$ approximates $u_z(t_n, z_i)$.

Next, the space derivatives are discretized. Therefore, standard finite differences are used. In order to simplify the spelling, the time index will be neglected. These leads to

$$u_{z,i} = \frac{u_{i+1} - u_{i-1}}{2\Delta z}, \quad (31)$$

$$\begin{aligned} h_z(u_{z,i}) &= \frac{h(u_{z,i+1}) - h(u_{z,i-1})}{2\Delta z} \\ &= \frac{1}{2\Delta z} \left\{ \frac{G_0}{1 + \left(\frac{\sqrt{3}}{2} \frac{|u_{i+2} - u_i|}{2\Delta z \gamma_{\text{ref}}} \right)^\beta} \frac{u_{i+2} - u_i}{2\Delta z} - \frac{G_0}{1 + \left(\frac{\sqrt{3}}{2} \frac{|u_i - u_{i-2}|}{2\Delta z \gamma_{\text{ref}}} \right)^\beta} \frac{u_i - u_{i-2}}{2\Delta z} \right\}, \end{aligned} \quad (32)$$

$$\begin{aligned} h_{zzz}(u_{z,i}) &= \frac{h(u_{z,i+2}) - 2h(u_{z,i+1}) + 2h(u_{z,i-1}) - h(u_{z,i-2})}{2\Delta z^3} \\ &= \frac{1}{2\Delta z^3} \left\{ \frac{G_0}{1 + \left(\frac{\sqrt{3}}{2} \frac{|u_{i+3} - u_{i+1}|}{2\Delta z \gamma_{\text{ref}}} \right)^\beta} \frac{u_{i+3} - u_{i+1}}{2\Delta z} \right. \\ &\quad - 2 \frac{G_0}{1 + \left(\frac{\sqrt{3}}{2} \frac{|u_{i+2} - u_i|}{2\Delta z \gamma_{\text{ref}}} \right)^\beta} \frac{u_{i+2} - u_i}{2\Delta z} + 2 \frac{G_0}{1 + \left(\frac{\sqrt{3}}{2} \frac{|u_i - u_{i-2}|}{2\Delta z \gamma_{\text{ref}}} \right)^\beta} \frac{u_i - u_{i-2}}{2\Delta z} \\ &\quad \left. - \frac{G_0}{1 + \left(\frac{\sqrt{3}}{2} \frac{|u_{i-1} - u_{i-3}|}{2\Delta z \gamma_{\text{ref}}} \right)^\beta} \frac{u_{i-1} - u_{i-3}}{2\Delta z} \right\}. \end{aligned} \quad (33)$$

Since Eq. (28) is nonlinear, a numerical scheme has to be used in order to calculate u_i^{n+1} iteratively. For this, Newton's method is used, for which the computation of the Jacobian matrix is necessary. The absolute value function $g(x) = |x|$ is weakly differentiable with $\text{sgn}(x)$ as weak derivative.

Using this and $\text{sgn}(x)x = |x|$, it follows

$$\begin{aligned}
\frac{\partial f}{\partial u_{i+3}}(u)(z_i) &= B_1 L^2 G_0 \frac{1 + (1 - \beta) \left(\frac{\sqrt{3}}{2} \frac{|u_{i+3} - u_{i+1}|}{2\Delta z \gamma_{\text{ref}}} \right)^\beta}{4\Delta z^4 \left(1 + \left(\frac{\sqrt{3}}{2} \frac{|u_{i+3} - u_{i+1}|}{2\Delta z \gamma_{\text{ref}}} \right)^\beta \right)^2}, \\
\frac{\partial f}{\partial u_{i-3}}(u)(z_i) &= B_1 L^2 G_0 \frac{1 + (1 - \beta) \left(\frac{\sqrt{3}}{2} \frac{|u_{i-1} - u_{i-3}|}{2\Delta z \gamma_{\text{ref}}} \right)^\beta}{4\Delta z^4 \left(1 + \left(\frac{\sqrt{3}}{2} \frac{|u_{i-1} - u_{i-3}|}{2\Delta z \gamma_{\text{ref}}} \right)^\beta \right)^2}, \\
\frac{\partial f}{\partial u_{i+2}}(u)(z_i) &= -G_0 \left(\Delta z^2 + B_2 \frac{\rho L^2 \Delta z^2}{G_0 \Delta t^2} + 2B_1 L^2 \right) \frac{1 + (1 - \beta) \left(\frac{\sqrt{3}}{2} \frac{|u_{i+2} - u_i|}{2\Delta z \gamma_{\text{ref}}} \right)^\beta}{4\Delta z^4 \left(1 + \left(\frac{\sqrt{3}}{2} \frac{|u_{i+2} - u_i|}{2\Delta z \gamma_{\text{ref}}} \right)^\beta \right)^2}, \\
\frac{\partial f}{\partial u_{i-2}}(u)(z_i) &= -G_0 \left(\Delta z^2 + B_2 \frac{\rho L^2 \Delta z^2}{G_0 \Delta t^2} + 2B_1 L^2 \right) \frac{1 + (1 - \beta) \left(\frac{\sqrt{3}}{2} \frac{|u_i - u_{i-2}|}{2\Delta z \gamma_{\text{ref}}} \right)^\beta}{4\Delta z^4 \left(1 + \left(\frac{\sqrt{3}}{2} \frac{|u_i - u_{i-2}|}{2\Delta z \gamma_{\text{ref}}} \right)^\beta \right)^2}, \\
\frac{\partial f}{\partial u_i}(u)(z_i) &= \frac{\rho}{\Delta t^2} - \frac{\partial f}{\partial u_{i+2}}(u)(z_i) - \frac{\partial f}{\partial u_{i-2}}(u)(z_i), \\
\frac{\partial f}{\partial u_{i+1}}(u)(z_i) &= -\frac{\partial f}{\partial u_{i+3}}(u)(z_i), \\
\frac{\partial f}{\partial u_{i-1}}(u)(z_i) &= -\frac{\partial f}{\partial u_{i-3}}(u)(z_i), \\
\frac{\partial f}{\partial u_j}(u)(z_i) &= 0 \quad \text{for } j < i - 3 \text{ and } j > i + 3.
\end{aligned} \tag{34}$$

In order to simulate the solution on an open domain, absorbing boundary conditions has been used. The numerical solution of the linear equation (13) using a finite difference scheme can be computed in a similar way. For details, see Appendix A.

5. Numerical results

In this section we show and discuss numerical results for the nonlinear Eq. (9) with the choice of parameters from Tab. 1.

G_0 [Pa]	ρ [kg m ⁻³]	β [-]	γ_{ref} [-]	B_1 [-]	B_2 [-]	L [m]
$111.86 \cdot 10^6$	2009.8	0.91	10^{-3}	1	1.78	0.2

Table 1: Medium parameter values.

5.1. Solution for the Gaussian pulse

First of all, the temporal evolution of a solution is studied, where as initial condition a Gaussian pulse is used, i. e.

$$u(t = 0, z) = u_0 \exp(-z^2/(2\sigma^2)). \quad (35)$$

Thereby, the amplitude $u_0 = 0.0128$ m and standard deviation $\sigma = 1$ m has been chosen. It has to be noted that a value of $u_0 = 0.0032$ m represents moderate earthquakes and $u_0 = 0.016$ m represents strong earthquakes. In order to compute the numerical solution by using the scheme described in sec. 5.2, an initial condition at time point t_{-1} , i. e. u^{-1} has to be chosen. In this study, $u^{-1} = u^0$ is used, resulting in a solution with zero initial velocity. The resulting numerical solution can be seen in Fig. 1. It is shown that the initial seismic wave divides into two parts, which propagate in the directions of the boundaries. We can also observe, that the nonlinear solution does not have sharp edges, which would be the case if the fourth order derivative terms were omitted in equation (9).

In order to see the effect of the nonlinear terms in Eq. (9), the temporal evolution of the corresponding solution for the linear case using Eq. (13) can be seen in Fig. 2. There is a clear difference between the linear and nonlinear solution. It can be seen that although the general behavior of the solution stays the same, the solution is now much higher and steeper compared to the nonlinear case. In order to make this more clear, Fig. 3 shows both solution at the end of the simulation time. It can be seen that the linear solution propagates faster, but small wave fluctuations appear. The nonlinear solution does not show this fluctuations, but has negative values during propagation.

In order to study the interaction of two solutions, two Gaussian pulses starting at $z_1 = -10$ m, $z_2 = 10$ m with amplitudes $u_1 = 0.0064$ m, $u_2 = 0.0128$ m and the same standard deviation $\sigma = 1$ m are considered. The corresponding initial condition has been calculated by adding both pulses and temporal evolution of the solution is shown in Fig. 5. It is shown that both pulses divided directly in two parts, propagating in different direction with a constant shape. Thereby, an interaction of the resulting waves does not destroy the structure of the each wave, but has less effect on them.

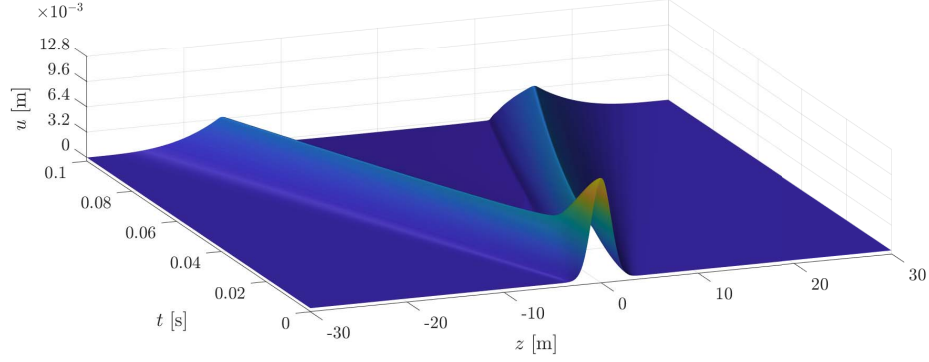


Figure 1: Solution of the nonlinear equation (9) with a Gaussian pulse as initial condition with an amplitude of $u_0 = 0.0128$ m.

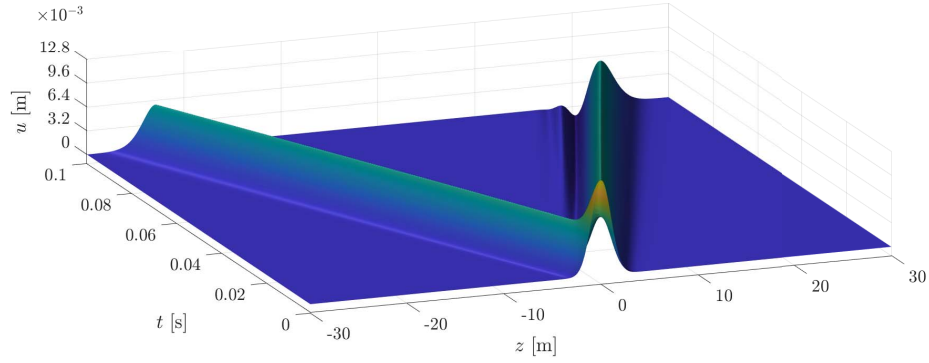


Figure 2: Solution of the linear equation (13) with a Gaussian pulse as initial condition with an amplitude of $u_0 = 0.0128$ m.

5.2. The stationary wave solutions

In order to compute the stationary wave solutions, we solve Eq. (22) numerically for $y = u_\xi$. Thereby, the traveling velocity c can be arbitrarily chosen. An integration with respect to ξ yields finally the solution u , which is used as initial condition for Eq. (9)

Figure 6 (a),(b) and Fig. 7 (a),(b) show the resulting phase plots and initial conditions for $c = 155$ m/s and $c = 100$ m/s, respectively.

In order to confirm that in fact stationary wave solutions for the used nonlocal, history-dependent nonlinear medium have been found, the above solutions of equation (22) are used as initial conditions for Eq. (9). Since

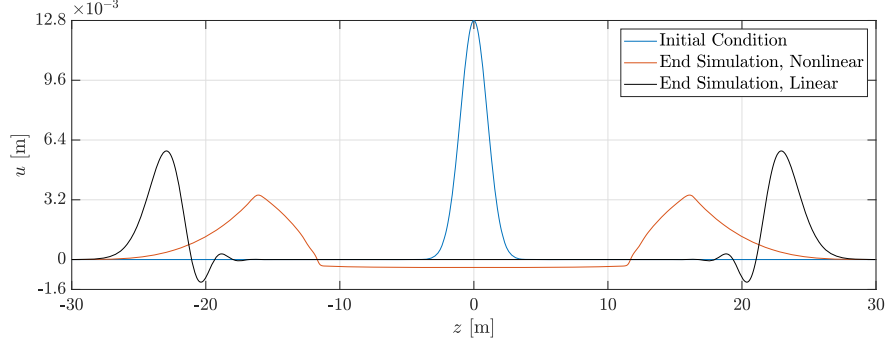


Figure 3: Comparison of the solution of the linear (9) and nonlinear (13) equation at the end of the simulation time. For both cases, the same initial condition has been used.

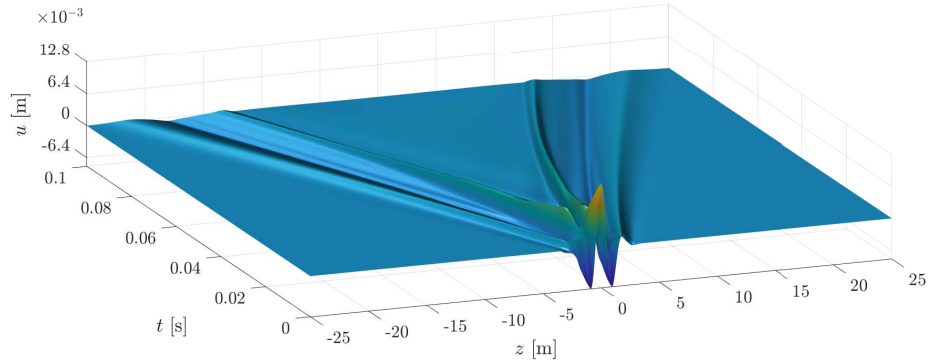


Figure 4: Solution of the nonlinear equation (9) with a Gaussian-Cosin pulse as initial condition with an amplitude of $u_0 = 0.0128$ m.

the scheme described in sec. 5.2 needs also an initial condition at the time point t^{-1} , the corresponding values at this time have to be computed as well. Because the stationary solution propagates with the velocity c , the solution u^{-1} at time point t^{-1} can be computed by shifting the stationary solution in space by ct^{-1} . The resulting solutions can be seen in Fig. 6 (c) and Fig. 7 (c), respectively. It can be observed that the solutions are not changing their shape in time. In order to clearly illustrate this, Fig. 6 (b) and 7 (b) show the space shifted initial condition with the corresponding solution at the end of the simulation time. Up to an numerical error, these solutions coincide. This confirms that stationary wave solutions for the used nonlocal, history-dependent nonlinear medium have been found.

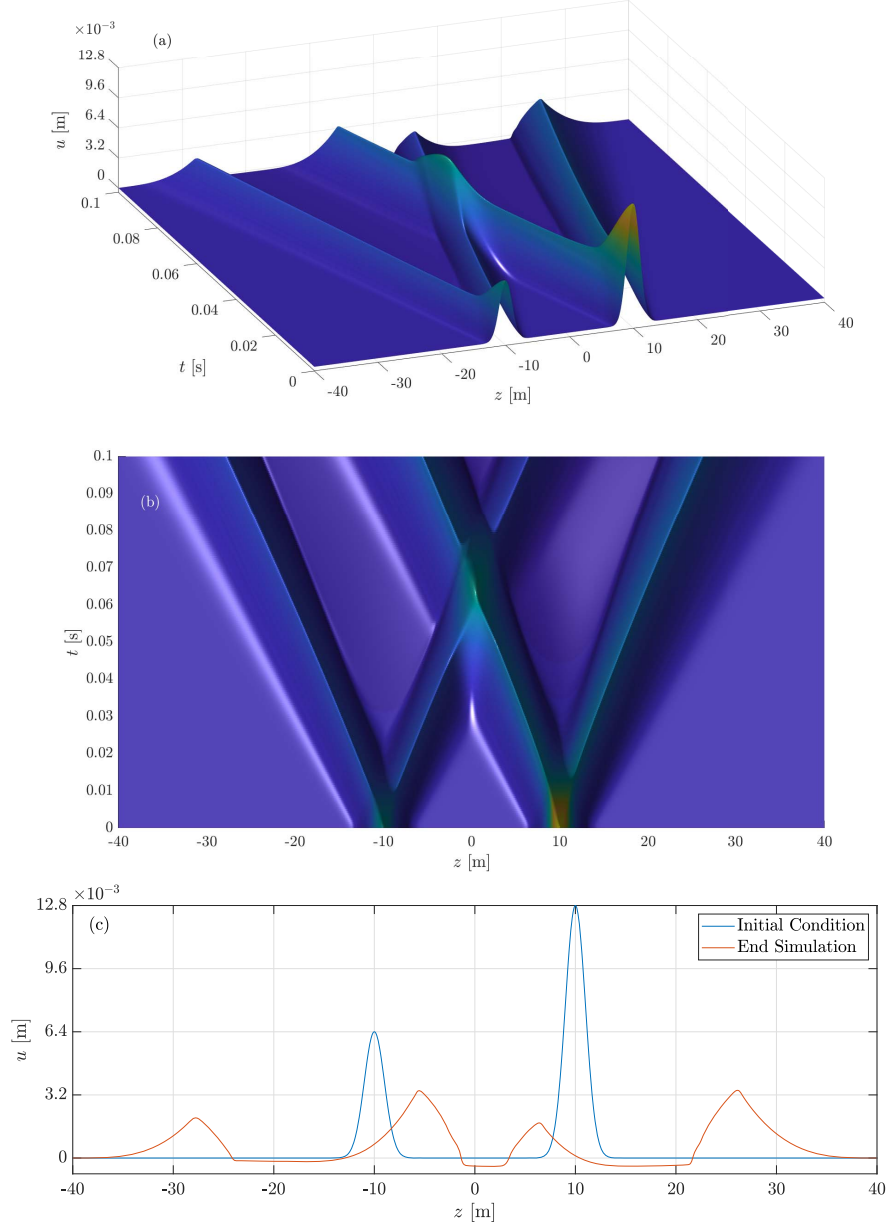


Figure 5: Interaction of two Gaussian pulses with maximal amplitudes $u_1 = 0.0064$ m and $u_2 = 0.0128$ m, starting at the positions $z_1 = -10$ m and $z_2 = 10$ m. The Solution is shown from two different perspectives ((a) and (b)) and at the end of the simulation time (c).

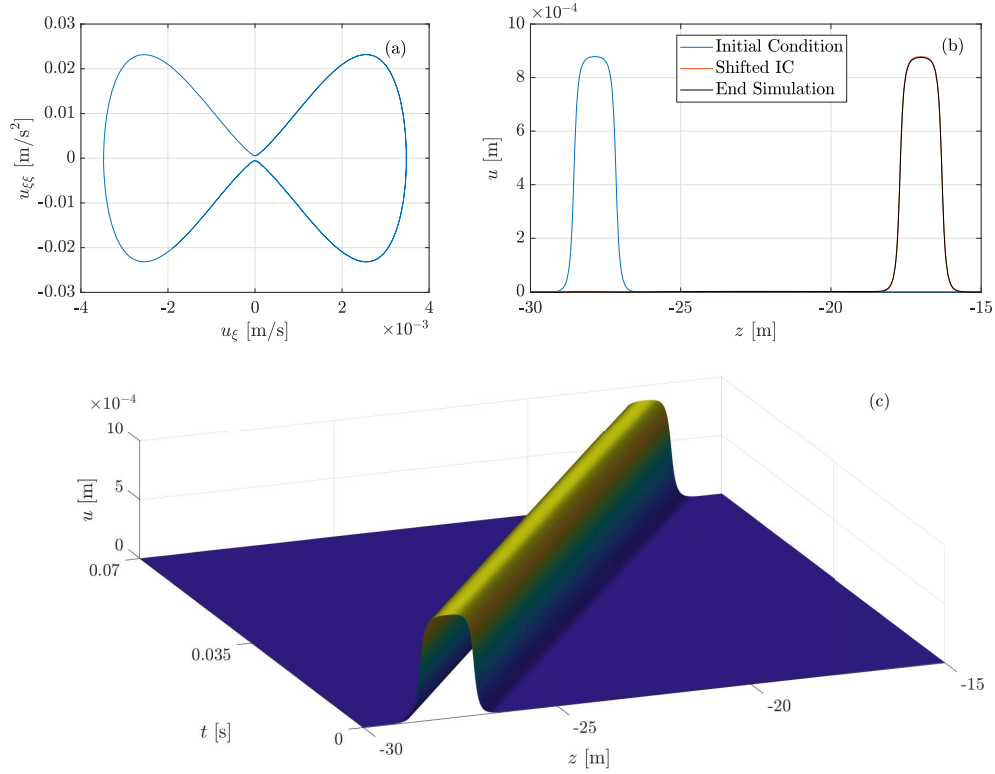


Figure 6: a: Phase plot. b: Initial condition (blue), initial condition shifted in space (red) and the solution at the end of the simulation time (black). c: Full time simulation. These results are for $c = 155 \text{ m/s}$.

Finally we were curious, whether the obtained stationary wave solutions are solitons. One property of solitons is, that they do not change their shape during propagation, such as the stationary solutions shown before. The second property is, that they do not change their shape after collision with each other. As can be see in Fig. 10, the first stationary solution for $c = 155$ changes its shape after a collision with the corresponding stationary solution with opposite direction of propagation. We have also computed a collision of our second stationary solution for c equals 100, which is shown in Fig. 11. We observe a very interesting nonlinear behaviour after collision, but also this solution is not a soliton. It remains an open question, whether it is possible to find solitary seismic waves.

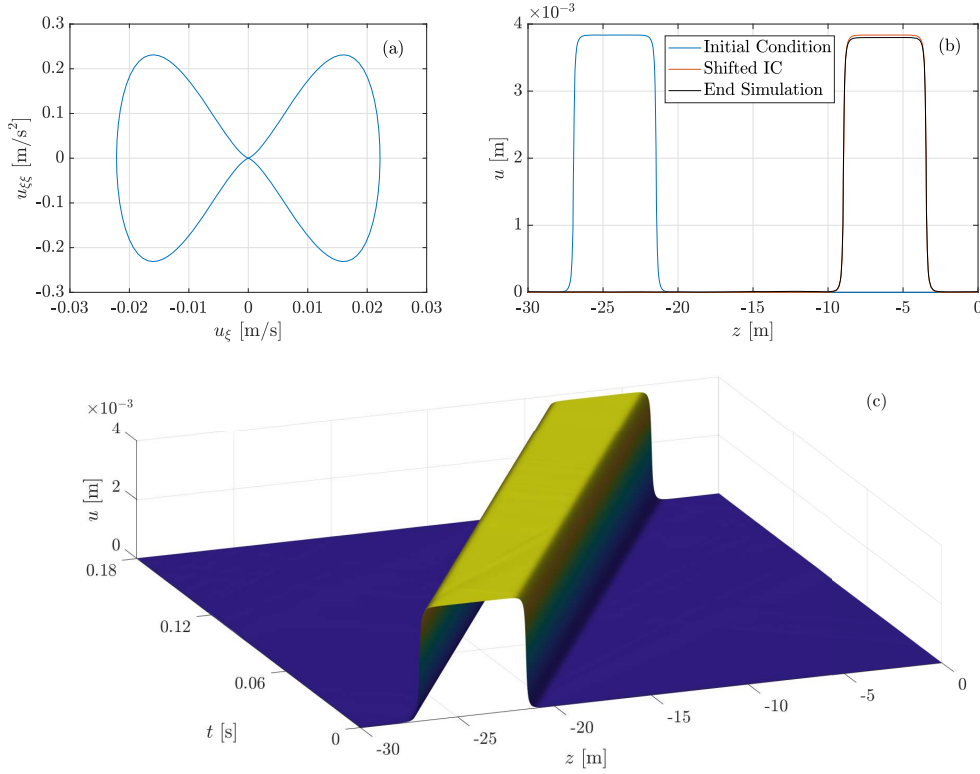


Figure 7: a: Phase plot. b: Initial condition (blue), initial condition shifted in space (red) and the solution at the end of the simulation time (black). c: Full time simulation. These results are for $c = 100 \text{ m/s}$.

6. Conclusions

In this work we have developed a new equation for nonlinear shear waves which takes into account nonlocality and history dependence by including higher order derivative terms. For this new nonlinear wave equation we have developed a numerical scheme with which we could compute different numerical solutions. A main result of our work is that we have determined stationary solutions for the developed nonlinear wave equation for seismic shear waves. Moreover, we have checked, whether the found stationary wave solutions are solitary wave solutions. It turned out, that these solutions do not keep their shape after collision with each other. Therefore, they are not solitary wave solutions. It will be interesting, whether solitary wave solutions can be found for seismic wave propagation in the future.

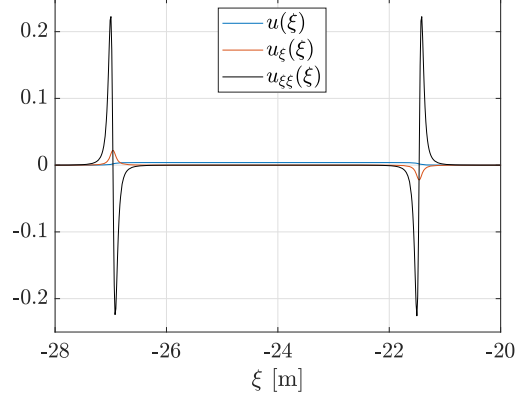


Figure 8: Stationary wave initial condition and the corresponding first and second derivative in ξ . These results are for $c = 100$ m/s.

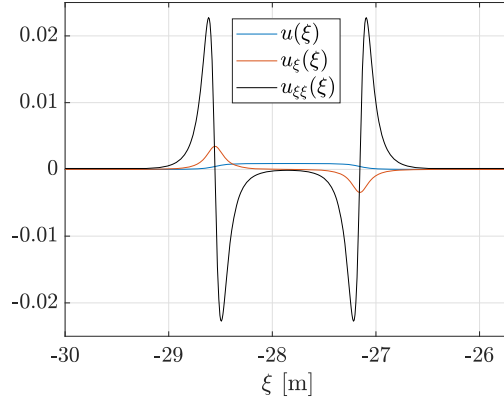


Figure 9: Stationary wave initial condition and the corresponding first and second derivative in ξ . These results are for $c = 155$ m/s.

Appendix A. Numerical schemes for linear Seismic waves

In order to solve eq. 13, a finite difference scheme is introduced. Using eq. 14, this equation can be expressed by

$$\rho u_{tt} = G_0 u_{zz} - B_1 L^2 G_0 u_{zzzz} + B_2 \rho L^2 u_{ttzz}. \quad (\text{A.1})$$

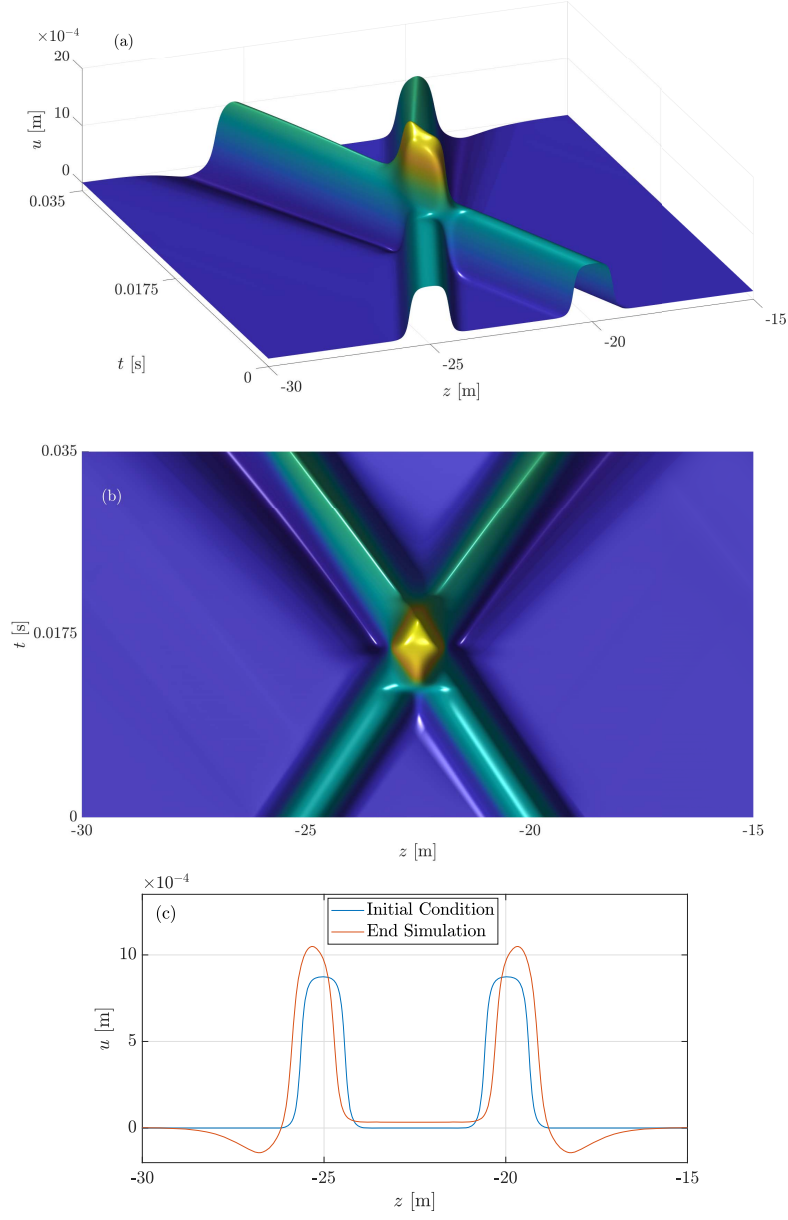


Figure 10: Interaction of two stationary wave solutions from two different points of view and the corresponding initial condition as well as the solution at the end of the simulation. These results are for $c = 155$ m/s.

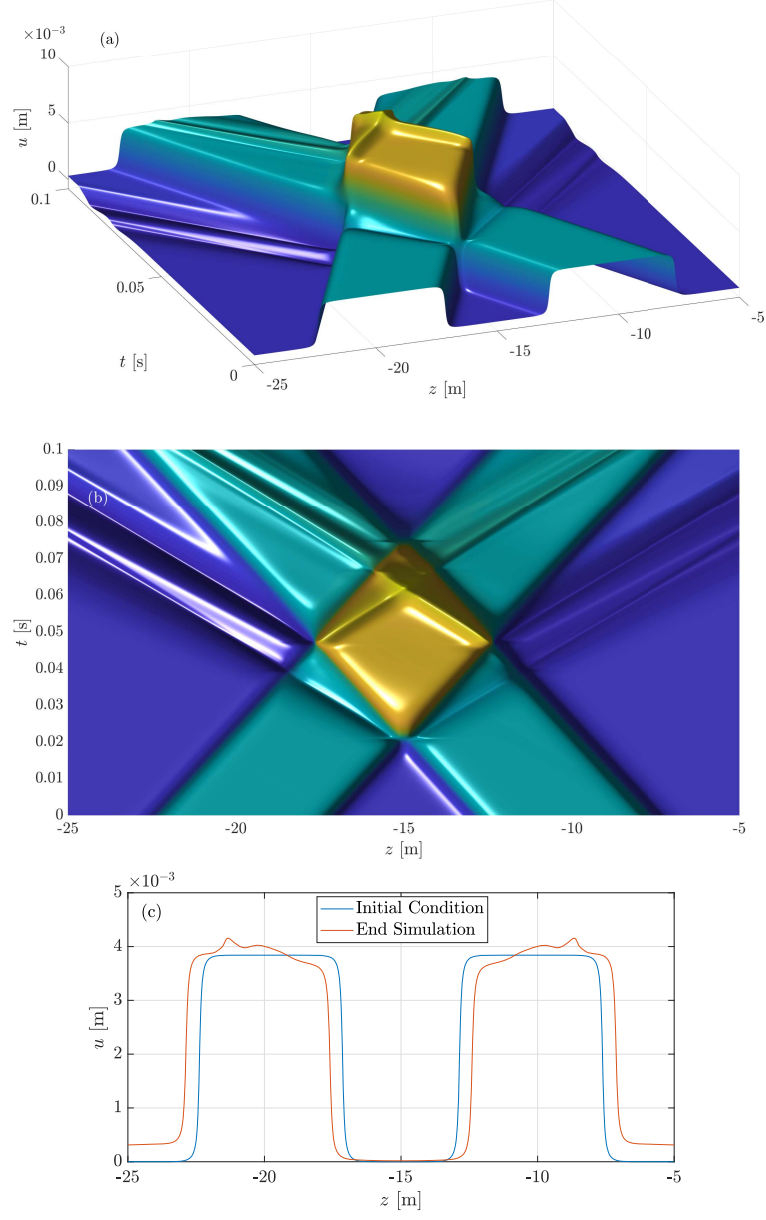


Figure 11: Interaction of two stationary wave solutions from two different points of view and the corresponding initial condition as well as the solution at the end of the simulation. These results are for $c = 100$ m/s.

Applying explicit finite difference approximations, this can be written as

$$\begin{aligned} \rho \frac{u_i^{n+1} - 2u_i^n + u_i^{n-1}}{\Delta t^2} = & \\ G_0 \frac{u_{i+1}^n - 2u_i^n + u_{i-1}^{n-1}}{\Delta z^2} - B_1 L^2 G_0 \frac{u_{i+2}^n - 4u_{i+1}^n + 6u_i^n - 4u_{i-1}^{n-1} + u_{i-2}^n}{\Delta z^4} & \\ + B_2 \rho L^2 \frac{u_{i+1}^{n+1} - 2u_i^{n+1} + u_{i-1}^{n+1} - 2u_{i+1}^n + 4u_i^n - 2u_{i-1}^n + u_{i+1}^{n-1} - 2u_i^{n-1} + u_{i-1}^{n-1}}{\Delta t^2 \Delta z^2}. & \end{aligned} \quad (\text{A.2})$$

Ordering all unknown values of u at the timepoint t^{n+1} at the left hand side and the rest at the right hand side leads into a linear system of equation, which has to be solved in each timestep. In order to simulate the solution in an open domain, absorbing boundary conditions have been used.

References

- [1] J. Régnier, L.-F. Bonilla, P.-Y. Bard, E. Bertrand, F. Hollender, H. Kawase, D. Sicilia, P. Arduino, A. Amorosi, D. Asimaki, et al., International benchmark on numerical simulations for 1d, nonlinear site response (prenolin): Verification phase based on canonical cases, Bulletin of the Seismological Society of America 106 (2016) 2112–2135.
- [2] Y. Hashash, C. Phillips, D. R. Groholski, Recent advances in non-linear site response analysis (2010).
- [3] S. L. Kramer, Geotechnical earthquake engineering, Prentice Hall, Upper Saddle River, New Jersey, 1996.
- [4] J. Zhang, E. Sulollari, A. B. Fărăgău, F. Pisanò, P. van der Male, M. Martinelli, A. V. Metrikine, K. N. van Dalen, Harmonic balance method for the stationary response of finite and semi-infinite nonlinear dissipative continua: Three canonical problems, in: Nonlinear Dynamics of Discrete and Continuous Systems, Springer, 2020, pp. 255–274.
- [5] A. Jeffrey, J. Engelbrecht, Nonlinear waves in solids, Springer, 1994.
- [6] A. Metrikine, On causality of the gradient elasticity models, Journal of Sound and Vibration 297 (2006) 727–742.

- [7] V. Y. Belashov, S. V. Vladimirov, Solitary waves in dispersive complex media: theory, simulation, applications, volume 149, Springer Science & Business Media, 2006.
- [8] A. C. Eringen, Nonlocal continuum field theories, Springer Science & Business Media, 2002.
- [9] A. Verruijt, An introduction to soil dynamics, volume 24, Springer Science & Business Media, 2009.
- [10] N. H. Polakowski, E. J. Ripling, Strength and structure of engineering materials (1966).
- [11] E. Benvenuti, A. Simone, One-dimensional nonlocal and gradient elasticity: closed-form solution and size effect, Mechanics Research Communications 48 (2013) 46–51.
- [12] B. O. Hardin, V. P. Drnevich, Shear modulus and damping in soils: measurement and parameter effects, Journal of Soil Mechanics & Foundations Div 98 (1972).
- [13] A. V. Metrikine, H. Askes, One-dimensional dynamically consistent gradient elasticity models derived from a discrete microstructure: Part 1: Generic formulation, European Journal of Mechanics-A/Solids 21 (2002) 555–572.
- [14] H. Georgiadis, I. Vardoulakis, G. Lykotrafitis, Torsional surface waves in a gradient-elastic half-space, Wave Motion 31 (2000) 333–348.